# Quantitative proteomic profiling of primary cancer-associated fibroblasts in oesophageal adenocarcinoma

Antigoni Manousopoulou[1#], Annette Hayden[2#], Massimiliano Mellone[2], Diana J. Garay-Baquero[3], Cory H. White[3&], Fergus Noble[2], Monette Lopez[4], Gareth J. Thomas[2], Timothy J. Underwood[2*] and Spiros D. Garbis[1,2*]

[1]Institute for Life Sciences, University of Southampton, Southampton, UK; [2]Cancer Sciences Unit, Faculty of Medicine, University of Southampton, Southampton, UK; [3]Clinical and Experimental Sciences Unit, Faculty of Medicine, University of Southampton, Southampton, UK; [4]University Hospital Southampton NHS Foundation Trust, Southampton, UK

[#]These authors contributed equally to the study

[&]Present address: Merck Exploratory Science Center, Cambridge MA USA

*SDG and TJU jointly led the study and are co-corresponding authors

**Corresponding authors:**

Spiros D. Garbis & Timothy J. Underwood

Cancer Sciences Unit, Faculty of Medicine

University of Southampton

SO16 6YD, Southampton, UK

Email: S.D.Garbis@soton.ac.uk; T.J.Underwood@soton.ac.uk

**Running title:** CAF proteomic profiling in OAC

**Keywords:** proteomics, iTRAQ, CAF, tumour microenvironment, myofibroblast, treatment targets

**Abstract** (200 words)

Background: Cancer–associated fibroblasts (CAFs) form the major stromal component of the tumour microenvironment (TME). The present study aimed to examine the proteomic profiles of CAFs vs. normal fibroblasts (NOFs) from patients with oesophageal adenocarcinoma to gain insight into their pro-oncogenic phenotype.

Methods: CAFs/NOFs from four patients were sub-cultured and analysed using quantitative proteomics. Differentially expressed proteins (DEPs) were subjected to bioinformatics and compared with published proteomics and transcriptomics datasets.

Results: Principal component analysis of all profiled proteins showed that CAFs had high heterogeneity and clustered separately from NOFs. Bioinformatics interrogation of the DEPs demonstrated inhibition of *Adhesion of Epithelial Cells*, *Adhesion of connective tissue cells* and *Cell death of Fibroblast Cell Lines* in CAFs vs. NOFs ($p < 0.0001$). KEGG pathway analysis showed a significant enrichment of the insulin-signalling pathway ($p = 0.03$). Gene ontology terms related with Myofibroblast phenotype, Metabolism, Cell adhesion/migration, Hypoxia/oxidative stress, Angiogenesis, Immune/inflammatory response were enriched in CAFs vs. NOFs. Nestin, a stem-cell marker up-regulated in CAFs vs. NOFs, was confirmed to be expressed in the TME with immunohistochemistry.

Conclusions: The identified pathways and participating proteins may provide novel insight on the tumour-promoting properties of CAFs and unravel novel adjuvant therapeutic targets in the TME.

## Introduction

Oesophageal cancer represents a significant global health burden with 395,000 deaths in 2010, an increase of nearly 15% from 1990 (Lozano *et al*, 2012). Oesophageal adenocarcinoma (OAC) is the predominant histological subtype in Western countries and age-standardised incidence rates are rising by 40% every 5 years (Lepage *et al*, 2008). The United Kingdom has the highest incidence of OAC in the world, and outcomes are poor because 60–70% of patients present with late-stage disease too advanced for treatment with curative intent (Arnold *et al*, 2014).

Using whole genome sequencing the OCCAMS consortium has identified new mutational signatures of OAC disease types that might be suitable for targeted treatments (Dulak *et al*, 2013; Ross-Innes *et al*, 2015; Weaver *et al*, 2014). However, findings from the OCCAMS cohorts require pre-clinical validation prior to implementation in trials, and studies are needed to understand the extent to which the genomic distinction is maintained downstream, at the level of the transcriptome and proteome (Secrier *et al*, 2016). Moreover, although mutationally corrupted cancer cells are recognized as the driving force of tumour development and progression, a key knowledge gap hindering the prediction of which patients will benefit from treatment is that the contribution of the tumour microenvironment (TME) is not considered (Hanahan and Coussens, 2012).

Our group's work has focused on the relationship between tumour cells and cancer-associated fibroblasts (CAFs), which form the major cellular component of the TME (De Wever *et al*, 2008). The in vivo "education" or "reprogramming" of fibroblasts by tumour cells is an established mechanism by which cancer cells exploit the plastic nature of reactive cell populations to generate a tumour-supportive microenvironment (Erez *et al*, 2010). The accumulation of CAFs in tumours correlates with poor prognosis across cancer types, including OAC, where we have shown that the presence of CAFs is more predictive of poor outcome than T, N or M stage (Marsh *et al*, 2011; Underwood *et al*, 2015). CAFs

84 are most commonly characterized by the acquisition of an “activated”, alpha-smooth
85 muscle actin (α-SMA) positive, myofibroblast phenotype (Marsh *et al*, 2011), which
86 regulates a number of tumour promoting processes (Underwood *et al*, 2015; Hanley *et al*,
87 2016). Additionally, CAFs may be implicated in the development of drug resistance during
88 chemotherapy treatment of cancer patients (Wang *et al*, 2017; Kalluri *et al*, 2006). Along
89 these lines, anti-cancer drugs have been found to become ineffective against cancer cells
90 co-cultured with various types of stromal cells (Straussman *et al*, 2012).

91 Shotgun proteomics, supported by recent technological advances in mass
92 spectrometry, is gradually becoming an indispensible analytical tool in cancer research
93 since the unbiased protein expression profiling of tumours or their microenvironment can
94 provide novel biological insight but also help identify novel diagnostic, prognostic and
95 therapeutic targets that can eventually influence clinical practice (Larkin *et al*, 2016;
96 Galanos *et al*, 2016; Hanley *et al*, 2016; Bouchal *et al*, 2015; Zeidan *et al*, 2015). There
97 are only a limited number of studies that have examined the global proteomic portrait of
98 primary CAFs derived from human cancer patients (Groessl *et al*, 2014; Fu *et al*, 2014,
99 Torres *et al*, 2015).

100 We have previously reported the shotgun proteomic analysis of primary, patient-
101 matched, CAF/NOF pairs (n=4) from patients with OAC (Hanley *et al*, 2016). The analysis
102 resulted in the profiling of 3,579 unique proteins, of which 172 were up- and 368 down-
103 regulated in CAFs vs. NOFs. The focus of the study by Hanley *et al*. was to examine the
104 relative expression levels of extracellular matrix proteins in CAFs vs. NOFs.

105 The aim of the present study was to apply a more in-depth proteomics
106 methodology in combination with comprehensive bioinformatics analysis to an additional
107 cohort of primary patient-matched CAF/NOF pairs (n=4) derived from patients with OAC in
108 order to gain insight into the pro-oncogenic features of the myofibroblast phenotype. An
109 additional aim was to identify novel therapeutic targets relevant to the TME. An overview
110 of the study workflow is presented in **Figure 1**.

111

## Materials and Methods

### Primary cell culture

Experimental protocols received ethical approval by the Southampton and South West Hampshire Research Ethics Committee (09/H0504/66). All participants signed an informed consent form. Fibroblasts were derived from four patients with oesophageal adenocarcinoma and sub-cultured as previously described (Underwood *et al*, 2015). Normal fibroblasts (NOFs) were taken from the proximal resection margin (at least 10 cm distant from the cancer) of each patient. Cell culture passage number was consistently under four.

### Quantitative proteomics sample processing

Cell pellets were snap frozen at -80 °C. These were dissolved in 0.5 M triethylammonium bicarbonate, 0.05% sodium dodecyl sulphate and subjected to pulsed probe sonication (Misonix, Farmingdale, NY, USA). Lysates were centrifuged (16,000 g, 10 min, 4oC) and supernatants were measured for protein content using infrared spectroscopy (Merck Millipore, Darmstadt, Germany). Lysates were then reduced, alkylated and subjected to trypsin proteolysis. Peptides were labelled using the eight-plex iTRAQ reagent kit (113=NOF patient 1, 114=NOF patient 2, 115= NOF patient 3, 116= NOF patient 4, 117= CAF patient 1, 118= CAF patient 2, 119= CAF patient 3, 121= CAF patient 4) and analysed using multi-dimensional liquid chromatography and tandem mass spectrometry.

### Two-dimensional LC-MS proteomic analysis

To enhance peptide separation efficiency and subsequent mass spectrometry analysis, the initial offline peptide fractionation was based on alkaline C4 Reverse Phase

(RP) chromatography (Kromasil 150 x 2.1 mm, 3.5 µm particle, 100Å pore size, Merck KGaA, Darmstadt, Germany) using gradient mobile phase conditions as previously reported by the authors (Manousopoulou *et al*, 2017). All other method details were as reported by the authors (Manousopoulou *et al*, 2016; Manousopoulou *et a*l, 2017).

**Database searching**

Unprocessed raw files were submitted to Proteome Discoverer 1.4 for target decoy searching against the UniProtKB homo sapiens database comprised of 20,159 entries (release date January 2015), allowing for up to two missed cleavages, a precursor mass tolerance of 10ppm, a minimum peptide length of six and a maximum of two variable (one equal) modifications of; iTRAQ 8-plex (Y), oxidation (M), deamidation (N, Q), or phosphorylation (S, T, Y). Methylthio (C) and iTRAQ (K, Y and N-terminus) were set as fixed modifications. FDR at the peptide level was set at <0.05. Percent co-isolation excluding peptides from quantitation was set at 50. Reporter ion ratios from unique peptides only were taken into consideration for the quantitation of the respective protein. Raw iTRAQ intensity values of unique peptides were median-normalized and $\log_2$ transformed. A Student's T-Test using the normalised raw iTRAQ intensity was performed to identify differentially expressed unique peptides between CAFs and NOFs. Significance was set at $p \leq 0.05$. A protein was considered to be differentially expressed in CAFs vs. NOFs when it had at least one differentially expressed unique peptide and a mean iTRAQ log2ratio of $\geq \pm 0.2$. In adherence to the Paris Publication Guidelines for the analysis and documentation of peptide and protein identifications (http://www.mcponline.org/site/misc/ParisReport_Final.xhtml), only proteins identified with at least two unique peptides were further subjected to bioinformatics. All mass spectrometry data have been deposited to the ProteomeXchange Consortium via PRIDE with the dataset identifier PXD005444.

**Bioinformatics analysis**

Principal component analysis using the $log_2$ratio of each sample over the mean of all samples was performed using the online tool ClustVis (http://biit.cs.ut.ee/clustvis/). DAVID (https://david.ncifcrf.gov/) was applied to differentially expressed proteins in order to identify over-represented gene ontology terms and KEGG pathways. Fisher exact corrected p-values ≤ 0.05 were considered significant. Subcellular localization of top up- and down-regulated proteins in CAF vs. NOF was manually assessed using ExPASy (www.expasy.org). The diseases and functions module of Ingenuity Pathway Analysis (IPA) (Qiagen, Hilden, Germany) was used to predict upstream biological processes activated or inhibited based on a combination of up- and down-regulated proteins observed. Biological processes with a Fisher's exact p-value < 0.05 and a false discovery rate score (z -score) of ≥ 2 or ≤ − 2 were considered significantly activated or inhibited respectively (Krämer *et al*, 2014; Al-Daghri *et al*, 2014).

**Comparison of DEPs with published proteomics and transcriptomics datasets**

DEPs were compared with our previously published proteomics dataset of primary CAFs/NOFs from patients with OAC (n=4) (Hanley *et al*, 2016). To define DEPs in this previous dataset, the exact same criteria as described above for the present study were used. Common DEPs in the two proteomics experiments were compared with a publically available transcriptomics dataset of laser-capture micro-dissected oesophageal stroma (n=44; 17 with intestinal metaplasia, 16 with dysplasia and 11 with adenocarcinoma) (NCBI/NIH; GEO; dataset ID: GSE19632).

***In silico* evaluation of the prognostic value of DEPs in OAC**

Proteins identified to be differentially expressed in CAFs vs. NOFs in both proteomics experiments were *in silico* evaluated for their prognostic value in OAC using PrognoScan (http://www.abren.net/PrognoScan/), a database of published cancer microarray experiments linking gene expression to patient prognosis (Mizuno *et al*, 2009).

196

197 **Immunohistochemical validation of key findings**

198 Immunohistochemical staining was performed in sections derived from a cohort of
199 183 OAC patients as previously described (Underwood *et al*, 2015). Briefly, sections of
200 thickness 5μm were taken from the recipient paraffin block for IHC staining. Primary
201 antibody dilution for polyclonal rabbit anti-human Nestin was 1:100 (DAKO no. M3515).
202 Slides were de-paraffinized with xylene and rehydrated with alcohol. Incubation in 3%
203 $H_2O_2$ (in deionized water) for 10 minutes was used to suppress endogenous peroxidase
204 activity. Slides were incubated in 1mM ethylenediaminetetraacetic acid (EDTA) for 15
205 minutes at 98°C and pH 8.0, allowing antigen retrieval. Tissue was sequentially incubated
206 in avidin, biotin, primary and biotinylated secondary antibody (at appropriate dilutions),
207 streptabidin biotin-peroxidase complexes and DAB (3-3′-diaminobenzidine). Cores were
208 counter-stained with Mayers Haematoxylin, dehydrated and mounted with DPX. The
209 automated immunostainer DAKO® Autostainer Link 48 (Cambridge, UK) was used in a
210 CPA-accredited cellular pathology department with the use of antibodies optimised to
211 national diagnostic standards (NEQAS).

212

213 **Results**

214

215 **Proteomic profiling of primary oesophageal fibroblasts**

216 We compared the global proteomic profiles of matched pairs of primary CAFs and
217 NOFs taken from oesophageal resections of four OAC patients in order to identify proteins
218 and pathways that may be responsible for the pro-oncogenic CAF phenotype and the poor
219 patient prognosis associated with the accumulation of CAFs in OAC. Proteomic analysis
220 resulted in the profiling of 7,718 unique protein groups (peptide FDR p-value<0.05)
221 (**Supplementary Table 1**), a substantial improvement of more than double the number of
222 profiled unique proteins compared to our previously published proteomics dataset.
223 Principal component analysis of all profiled proteins demonstrated the more homogeneous

NOF phenotype clustered separately from that of the more heterogeneous CAFs (**Figure 2A**).

The differentially expressed proteome (DEP) comprised 699 up- and 987 down-regulated proteins in CAFs compared to NOFs (**Supplementary Table 2**). A volcano plot representation of the mean iTRAQ $log_2$ratio of proteins in CAF vs. NOF plotted against the minus log10(p-value) is presented in **Figure 2B**. Alpha-SMA expression was found to be variable but with a mean $log_2$ratio of 0.2 ± 0.9 (p-value<0.0001 at the peptide level) across all CAFs vs. NOFs examined (**Figure 2C**).

**Comparison of DEPs with published proteomics and transcriptomics datasets**

Of the DEPs, 136 proteins were also identified with the same trend of modulation in our previously published proteomic analysis of an independent primary CAF/NOF cohort from patients with OAC (Hanley *et al*, 2016) and the expression trend of five up- and 11 down-regulated proteins was confirmed in the publically available microarray dataset of OAC micro-dissected stromal cells. These proteins are presented in heatmap format in **Figure 2D**. Proteins identified in both proteomic experiments and confirmed with the same trend of modulation in the microarray dataset are highlighted in grey (**Figure 2D**). Among the proteins identified in both proteomics and confirmed at the transcriptomics dataset to be up-regulated in CAFs vs. NOFs were α-smooth muscle actin, lamin A (LMNA) and actin-1 (ACTN1).

**Bioinformatics Analysis**

The diseases and functions module of IPA predicted, based on the downstream up- and down-regulated proteins, that *Adhesion of Epithelial Cells* (z-score = - 2.4 | p=6.3E-06), *Adhesion of connective tissue cells* (z-score = - 2.3 | p=1.8E-05) and *Cell death of Fibroblast Cell Lines* (z-score = - 2.2 | p=1.7E-09) were significantly inhibited in CAFs vs. NOFs (**Figure 3A**). KEGG pathway analysis using DAVID showed a significant enrichment of the insulin-signalling pathway (Fisher exact p-value= 0.03 for the common

proteins between the two proteomics experiments and 0.05 for the DEPs analysed in the present study) (**Figure 3B**).

DAVID gene ontology analysis, accounting for both up- and down- regulated proteins constituting the DEP, demonstrated that processes related with *Myofibroblast phenotype*, *Metabolism*, *Cell adhesion/migration*, *Hypoxia/oxidative stress*, *Angiogenesis*, and *Immune/inflammatory response* were over-represented (**Figure 4A**). The top 10 up- and down-regulated proteins mapping to each GO term group are presented in heatmap format in **Figure 4B**. The sub-cellular localization of these proteins is also presented in the heatmap. Top up-regulated proteins that are either secreted or localized in the membrane are highlighted in the heatmap as potential therapeutic targets in CAF (gene names of the respective proteins are: CD9, MIF, HMGB2, HMGB1, CSPG4, CACNB3, APC, BCAM, CD97, LPP, LCT, TJP2, PLCD3, SLC9A3R1, CAV1, RAPGEF2, MAP3K7 and CD44) (**Figure 4B**).

### ***In silico*** **evaluation of the prognostic value of Nestin in OAC**

Using the *in silico* PrognoScan meta-analysis microarray database for the common DEPs in both proteomics experiments, increased levels of nestin was found to be associated with poor OAC patient prognosis [COX p-value=0.003; HR (95% CI) = 78.0 (4.3 to 1409.8)] (**Figure 5A**). Immunohistochemical staining of nestin was performed in a well-described cohort of 183 oesophageal tumours where the presence of α-SMA positive CAFs correlated strongly with poor overall survival (Underwood *et al*, 2015). The patient clinico-pathological characteristics of this cohort have been reported before (Underwood *et al*, 2015). Nestin showed a conserved expression pattern in the tumour microenvironment of OAC, being confined to CAF, blood vessels and smooth muscle cells. Example staining is shown in **Figure 5B**.

## Discussion

The seminal work of Paget over a century ago proposed that cancer cells constitute the "seeds" that colonize a favourable stromal microenvironment as the receptive "soil" (Han *et al*, 2015; Baulida *et al*, 2017). A key "soil" constituent is the normal fibroblast that acquires a cancerous phenotype by the "seed" cancer cell to facilitate its proliferation, invasion, and metastasis (Martin *et al*, 2011). However, the proteomic characterization of such cancer fibroblasts remains limited.

To address this need, our study made use of a comprehensive quantitative proteomics approach (**Figure 1**) and reports the most extensive proteome coverage to date of primary CAF/NOF pairs from patients with OAC, a considerable improvement in proteome coverage compared to our published CAF/NOF dataset. Principal Component Analysis (PCA) against the reporter ion ratios of the 7,718 unique protein analysed across all samples resulted in distinct molecular clusters for CAFs relative to NOFs (**Figure 2A**). In keeping with previous findings (Ishii *et al*, 2016; Underwood *et al*, 2015), PCA analysis showed marked heterogeneity in proteome expression for CAF relative to the more homogeneous proteome expression for NOF. Significant differential expression was observed for 699 up- and 987 down-regulated proteins across all CAFs relative to all NOFs, as highlighted in the volcano plot of **Figure 2B** ($log_2$ratio ≥ 0.2, p ≤ 0.05, t-test). Alpha-SMA (ACTA2) was analysed to be marginally up-regulated in CAFs vs. NOFs (as illustrated in the volcano plot of **Figure 2B**) ($log_2$ratio = 0.2 ±0.9; p-value<0.0001 at the peptide level) (**Figure 2C**). By contrast, our quantitative proteome revealed a large spectrum of novel proteins exhibiting a higher and more consistent level of differential expression that may constitute more robust candidate markers of the CAF phenotype (**Figure 2B** and **2C**, **Supplementary Table 2**). Consistent protein differential expression of CAF canonical markers was observed between the current quantitative proteome, a proteomics dataset reported by the authors (Hanley *et al*, 2016) and a publically available transcriptomics microarray dataset (**Figure 2D**). Notable surrogate markers of the CAF phenotype include the up-regulated proteins lamin A (LMNA) and actin-1 (ACTN1). LMNA has been implicated in the modulation of TGF-β1 on collagen production and

306 mesenchymal differentiation (Van Berlo *et a*l, 2005), and ACTN1 up-regulation has been
307 described in stromal fibroblasts derived from oral cancers (Chatzistamou *et al*, 2011).
308 The diseases and functions module of IPA predicted the *inhibition of Adhesion of*
309 *Epithelial Cells* (z-score = - 2.4 | p=6.3E-06) and *Adhesion of connective tissue cells* (z-
310 score = - 2.3 | p=1.8E-05) (**Figure 3A**). The inhibition of these processes suggests the
311 involvement of CAFs on increasing the tumour's metastatic potential. These findings
312 confirm and extend the current knowledge of the CAF phenotype also affecting cell
313 adhesion/cell migration processes (Underwood *et al*, 2015; Hanley *et al*, 2016).
314 Of relevance, given the endoergic character of increased cellular proliferation and
315 pro-metastatic phenotypes observed, the insulin-signalling pathway was significantly
316 enriched in the DEP of the present study as well as the common proteins with our
317 previously published proteomics dataset (**Figure 3B**). Increased expression of the insulin-
318 like growth factor 1 (IGF-I) and its receptor (IGF-IR) has been found to be associated with
319 tumour progression and poor prognosis in different cancer types including gastrointestinal
320 tumours (Giovannucci *et a*l, 2001; Woodson *et a*l, 2004). The tumour promoting properties
321 of IGF-IR are dependent on the activation of the down-stream insulin receptor substrates
322 (IRS) (Chan *et al*, 2008; Ramocki *et al*, 2008). IGF-I also plays a key role in the autocrine
323 and paracrine induction of CAF "activation" (Kalluri *et al*, 2006). A recent study showed
324 that NT157, an inhibitor of the IGF-IR-IRS signalling pathway, resulted in inhibition of CAF
325 "activation", as well as reduced expression of pro-oncogenic chemokines, cytokines and
326 growth factors, including several interleukins (IL-6, IL-11, IL-23) and TGFβ (Sanchez-
327 Lopez *et al*, 2016). The de-regulation of the insulin signalling pathway in CAFs could also
328 be linked to the "Reverse Warburg effect", a model describing the metabolic coupling
329 between stromal and cancer cells (Pavlides *et al*, 2009). One interesting protein mapping
330 in the insulin-signalling pathway was hexokinase-1 (HK1). HK1 was consistently
331 upregulated in both proteomic experiments and further confirmed at the microarray dataset
332 (**Figures 2D** and **3B**). HK1 catalyzes the first obligatory and rate-limiting step of glucose
333 metabolism, more specifically the phosphorylation of glucose to G6P (Smith, 2000).

Furthermore, HK1 has been suggested to regulate cell death, a process associated with abnormal proliferation and tumorigenesis (Pastorino and Hoek, 2003). HK1 has also been found to be upregulated in different cancer types, including kidney and breast carcinomas (Hooft *et al*, 2005; Millon *et al*, 2011). Furthermore, a recent study showed that HK1 over-expression is associated with poor patient prognosis in colorectal cancer (He *et al*, 2016). HK1 expression in CAFs and its implication with tumour aggressiveness warrants further investigation.

DAVID GO analysis identified terms related with *Myofibroblast phenotype*, *Metabolism*, *Cell adhesion/migration*, *Hypoxia/oxidative stress (*including *DNA damage response)*, *Angiogenesis*, and *Immune/inflammatory response* processes to be over-represented in the DEPs (**Figures 4A**). The gene names of the top-10 differentially expressed proteins observed for each these processes, including those classified as secreted or membrane associated, constitute novel observations and may reveal candidate therapeutic targets (**Figure 4B**).

Hypoxia, oxidative stress and DNA damage response were significantly enriched GO terms. Oxidation-reduction is an established process in CAFs (Balliet *et al*, 2011; Martin *et al*, 2011). CAFs have been shown to overproduce reactive oxygen species (ROS), leading to oxidative stress, inflammation and significant cellular damage, which could in turn affect DNA damage response (Martin *et al*, 2011; Trinchieri, 2012). The over-production of ROS by CAFs can induce oxidative stress in normal fibroblasts that further triggers CAF activation, thus leading to a positive feedback loop between ROS production and CAF activation (Jeziersdka-Drutel *et al*, 2013; Chan *et al*, 2017). Furthermore, the *Cell death of Fibroblast Cell Line* process was found to be inhibited (z-score = - 2.2 | p=1.7E-09), showing that CAFs may evade apoptosis possibly as a result of their enhanced DNA damage response.

Immune and inflammatory responses were also significantly over-represented terms in CAFs vs. NOFs (**Figure 4A**). Previous studies have reported on the immunomodulatory effects of CAF (Takahashi *et al*, 2017; Wen *et al*, 2017; Yeh *et al*,

2016). Specific pathways and their participatory proteins responsible for the interplay between CAF and the host immune response may be of relevance to a number of current clinical trials using immune checkpoint inhibitors in unselected patients with OAC. The success rate of these therapies may not depend entirely on the immune system, but also implicate CAF-induced alterations of the tumour microenvironment in preventing immune cell entry. This may warrant the combined use of immunotherapy and CAF permeability modifiers (Hanley *et al*, 2018). At the same token, CAFs have been reported to promote angiogenesis through different mechanisms, including ECM remodelling, recruitment of epithelial progenitor cells, and increased leucocyte infiltration through chemokine secretion, that in turn produce angiogenic factors (Tao *et al*, 2017).

An up-regulated protein identified in both proteomics experiments was nestin. Nestin was further investigated as it was found to correlate with decreased overall survival in patients with oesophageal cancer based on the *in silico* microarray meta-analysis tool PrognoScan (**Figure 5A**), suggesting that nestin may play an important role in OAC biology. Nestin is an intermediate filament protein originally detected in neuronal stem cells during development (Lendahl *et al*, 1990). Nestin has been detected in various types of solid tumours, including mesenchymal tumours and cancers (e.g. breast, lung, ovarian and gastrointestinal) (Ishiwata *et al*, 2011). Nestin has been suggested as a stem-cell marker indicating an undifferentiated and thus more invasive phenotype of transformed cells (Neradil *et al*, 2015). Immunohistochemical staining showed that nestin protein expression was confined to the tumour microenvironment of OAC (**Figure 5B**). A recent study showed that nestin suppression reduced the metastatic potential of endometrial cancer cells by inhibiting the TGFβ signalling cascade (Bokhari *et al*, 2016), the main pathway promoting aberrant CAF “activation” (Hawinkels *et al*, 2014).

The main study limitation is that only four matched pairs of fibroblasts were used to generate the proteomic expression profiles. This is partly compensated, however, by the evaluation of the analysed proteins using our previously published proteomics dataset (n=4) and an independent microarray dataset (n=44).

In conclusion, this study reports the proteomic profiling of primary CAFs from patients with OAC, a cancer with a vast unmet clinical need. The biological pathways and networks observed for the primary CAFs examined were found to emulate all the intrinsic hallmarks of cancer, as expected given the strong functional cross-talk between fibroblasts and cancer cells. Furthermore, the participating proteins to these biological processes may constitute novel adjuvant therapeutic targets for OAC in the TME as part of precision medicine protocols.

## References


Al-Daghri NM, Al-Attas OS, Johnston HE, Singhania A, Alokail MS, Alkharfy KM *et al*. Whole serum 3D LC-nESI-FTMS quantitative proteomics reveals sexual dimorphism in the milieu intérieur of overweight and obese adults. *J Proteome Res* 2014; **13**: 5094-105.

Arnold M, Soerjomataram I, Ferlay J, Forman D. Global incidence of oesophageal cancer by histological subtype in 2012. *Gut* 2014; **64**: 381-7.

Balliet RM, Capparelli C, Guido C, Pestell TG, Martinez-Outschoorn UE, Lin Z *et al.* Mitochondrial oxidative stress in cancer-associated fibroblasts drives lactate production, promoting breast cancer tumor growth: understanding the aging and cancer connection. *Cell Cycle* 2011; **10**: 4065-73.

Baulida J. Epithelial-to-mesenchymal transition transcription factors in cance-associated fibroblasts. *Mol Oncol* 2017; **11**: 847-59.

Bokhari AA, Baker TM, Dorjbal B, Waheed S, Zahn CM, Hamilton CA *et al.* Nestin suppression attenuates invasive potential of endometrial cancer cells by downregulating TGF-β signaling pathway. *Oncotarget* 2016; **7**: 69733-48.

418 Bouchal P, Dvořáková M, Roumeliotis T, Bortlíček Z, Ihnatová I, Procházková I *et al.*
419 Combined Proteomics and Transcriptomics Identifies Carboxypeptidase B1 and
420 Nuclear Factor κB (NF-κB) Associated Proteins as Putative Biomarkers of
421 Metastasis in Low Grade Breast Cancer. *Mol Cell Proteomics* 2015; **14**: 1814-30.
422 Chan BT, Lee AV. Insulin receptor substrates (IRSs) and breast tumorigenesis. *J*
423 *Mammary Gland Biol Neoplasia* 2008; **13**: 415–22.
424 Chan JS, Tan MJ, Sng MK, Teo Z, Phua T, Choo CC *et al.* Cancer-associated fibroblasts
425 enact field cancerization by promoting extratumoral oxidative stress. *Cell Death Dis*
426 2017; **8**: e2562.
427 Chatzistamou I, Dioufa N, Trimis G, Sklavounou A, Kittas C, Kiaris H *et al.* p21/waf1 and
428 smooth-muscle actin α expression in stromal fibroblasts of oral cancers. *Cell*
429 *Oncol (Dordr)* 2011; **34**: 483-8.
430 De Wever O, Demetter P, Mareel M, Bracke M. Stromal myofibroblasts are drivers of
431 invasive cancer growth. *Int J Cancer* 2008; **123**: 2229-38.
432 Dulak AM, Stojanov P, Peng S, Lawrence MS, Fox C, Stewart C *et al.* Exome and whole-
433 genome sequencing of esophageal adenocarcinoma identifies recurrent driver
434 events and mutational complexity. *Nat Genet* 2013; **45**: 478-86.
435 Erez N, Truitt M, Olson P, Arron ST, Hanahan D. Cancer-Associated Fibroblasts Are
436 Activated in Incipient Neoplasia to Orchestrate Tumor-Promoting Inflammation in
437 an NF-kappaB-Dependent Manner. *Cancer Cell* 2010; **17**: 135-47.
438 Fu Z, Song P, Li D, Yi C, Chen H, Ruan S, *et al.* Cancer-associated fibroblasts from
439 invasive breast cancer have an attenuated capacity to secrete collagens. *Int J*
440 *Oncol* 2014; **45**: 1479-88.
441 Galanos P, Vougas K, Walter D, Polyzos A, Maya-Mendoza A, Haagensen EJ, *et al.*
442 Chronic p53-independent p21 expression causes genomic instability by
443 deregulating replication licensing. *Nat Cell Biol* 2016; **18**: 777-89.
444 Giovannucci E. Insulin, insulin-like growth factors and colon cancer: a review of the
445 evidence. *J Nutr* 2001; **131**: 3109S–20S.

446 Groessl M, Slany A, Bileck A, Gloessmann K, Kreutz D, Jaeger W, *et al.* Proteome
447 profiling of breast cancer biopsies reveals a wound healing signature of cancer-
448 associated fibroblasts. *J Proteome Res* 2014; **13**: 4773-82.
449 Han Y, Zhang Y, Jia T, Sun Y. Molecular mechanisms underlying the tumor-promoting
450 functions of carcinoma-associated fibroblasts. *Tumor Biol* 2015; **36**: 1385-94.
451 Hanahan D, Coussens LM. Accessories to the crime: functions of cells recruited to the
452 tumor microenvironment. *Cancer Cell* 2012; **21**: 309-22.
453 Hanley CJ, Noble F, Ward M, Bullock M, Drifka C, Mellone M, *et al.* A subset of
454 myofibroblastic cancer-associated fibroblasts regulate collagen fiber elongation,
455 which is prognostic in multiple cancers. *Oncotarget* 2016; **7**: 6159-74.
456 Hanley CJ, Mellone M, Ford K, Thirdborough SM, Mellows T, Frampton SJ, *et al.*
457 Targeting the Myofibroblastic Cancer-Associated Fibroblast Phenotype Through
458 Inhibition of NOX4. *J Natl Cancer Inst* 2018; **110**: doi 10.1093/jnci/djx121.
459 Hawinkels LJ, Paauwe M, Verspaget HW, Wiercinska E, van der Zon JM, van der Ploeg K,
460 *et al.* Interaction with colon cancer cells hyperactivates TGF-beta signaling in
461 cancer-associated fibroblasts. *Oncogene 2014;* **33**: 97-107.
462 He X, Lin X, Cai M, Zheng X, Lian L, Fan D, *et al.* Overexpression of Hexokinase 1 as a
463 poor prognosticator in human colorectal cancer. *Tumour Biol* 2016; **37**: 3887-95.
464 Hooft L, van der Veldt AA, van Diest PJ, Hoekstra OS, Berkhof J, Teule GJ, *et al.*
465 [18F]fluorodeoxyglucose uptake in recurrent thyroid cancer is related to hexokinase
466 i expression in the primary tumor. *J Clin Endocrinol Metab* 2005; **90**: 328–34.
467 Ishii G, Ochiai A, Neri S. Phenotypic and functional heterogeneity of cancer-associated
468 fibroblast within the tumor microenvironment. *Adv Drug Deliv Rev* 2016; **99**: 186-
469 96.
470 Ishiwata T, Matsuda Y, Naito Z. Nestin in gastrointestinal and other cancers: effects on
471 cells and tumor angiogenesis. *World J Gastroenterol* 2011; **17**: 409–18

472 Jezierska-Drutel A, Rosenzweig SA, Neumann CA. Role of oxidative stress and the
473 microenvironment in breast cancer development and progression. *Adv Cancer Res*
474 2013; **119**: 107-25.
475 Kalluri R, Zeisberg M. Fibroblasts in cancer. *Nat Rev Cancer* 2006; **6**: 392-401.
476 Krämer A, Green J, Pollard J Jr, Tugendreich S. Causal analysis approaches in Ingenuity
477 Pathway Analysis. *Bioinformatics* 2014; **30**: 523-30.
478 Larkin SE, Johnston HE, Jackson TR, Jamieson DG, Roumeliotis TI, Mockridge CI, *et al.*
479 Detection of candidate biomarkers of prostate cancer progression in serum: a
480 depletion-free 3D LC/MS quantitative proteomics pilot study. *Br J Cancer* 2016;
481 **115**: 1078-1086.
482 Lendahl U, Zimmerman LB, McKay RD. CNS stem cells express a new class of
483 intermediate filament protein. *Cell* 1990; **60**: 585–95
484 Lepage C, Rachet B, Jooste V, Faivre J, Coleman MP. Continuing rapid increase in
485 esophageal adenocarcinoma in England and Wales. *Am J Gastro*enterol 2008;
486 **103**: 2694-9.
487 Lozano R, Naghavi M, Foreman K, Lim S, Shibuya K, Aboyans V, *et al.* Global and
488 regional mortality from 235 causes of death for 20 age groups in 1990 and 2010: a
489 systematic analysis for the Global Burden of Disease Study 2010. *Lancet* 2012;
490 **380**: 2095-128.
491 Manousopoulou A, Koutmani Y, Karaliota S, Woelk CH, Manolakos ES, Karalis K, *et al.*
492 Hypothalamus proteomics from mouse models with obesity and anorexia reveals
493 therapeutic targets of appetite regulation. *Nutr Diabetes* 2016; **6**: e204.
494 Manousopoulou A, Gatherer M, Smith C, Nicoll JAR, Woelk CH, Johnson M, *et al.*
495 Systems proteomic analysis reveals that clusterin and tissue inhibitor of
496 metalloproteinases 3 increase in leptomeningeal arteries affected by cerebral
497 amyloid angiopathy. *Neuropathol Appl Neurobiol* 2017; **43**: 492-504.

498 Marsh D, Suchak K, Moutasim KA, Vallath S, Hopper C, Jerjes W, *et al.* Stromal features
499 are predictive of disease mortality in oral cancer patients. *J Pathol* 2011; **223**: 470-
500 81.
501 Martin OA, Redon CE, Nakamura AJ, Dickey JS, Georgakilas AG, Bonner WM. Systemic
502 DNA damage related to cancer. *Cancer Res* 2011; **71**: 3437-41.
503 Millon SR, Ostrander JH, Brown JQ, Raheja A, Seewaldt VL, Ramanujam N. Uptake of 2-
504 NBDG as a method to monitor therapy response in breast cancer cell lines. *Breast*
505 *Cancer Res Treat* 2011; **126**: 55-62.
506 Mizuno H, Kitada K, Nakai K, Sarai A. PrognoScan: a new database for meta-analysis of
507 the prognostic value of genes. *BMC Med Genomics* 2009; **2**: 18.
508 Neradil J, Veselska R. Nestin as a marker of cancer stem cells. *Cancer Sci* 2015; **106**:
509 803-11.
510 Pastorino JG, Howek JB. Hexokinase II: the integration of energy metabolism and control
511 of apoptosis. *Curr Med Chem* 2003; **10**: 1535-51.
512 Pavlides S, Whitaker-Menezes D, Castello-Cros R, Flomenberg N, Witkiewicz AK, Frank
513 PG, *et al.* The reverse Warburg effect: aerobic glycolysis in cancer associated
514 fibroblasts and the tumor stroma. *Cell Cycle* 2009; **8**: 3984-4001.
515 Ramocki NM, Wilkins HR, Magness ST, Simmons JG, Scull BP, Lee GH, *et al.* Insulin
516 receptor substrate-1 deficiency promotes apoptosis in the putative intestinal crypt
517 stem cell region, limits Apcmin/+ tumors, and regulates Sox9. *Endocrinology 2008;*
518 **149**: 261-7.
519 Ross-Innes CS, Becq J, Warren A, Cheetham RK, Northen H, O'Donovan M, *et al.* Whole-
520 genome sequencing provides new insights into the clonal architecture of Barrett's
521 esophagus and esophageal adenocarcinoma. *Nat Genet* 2015; **47**: 1038-46.
522 Sanchez-Lopez E, Flashner-Abramson E, Shalapour S, Zhong Z, Taniguchi K, Levitzki A,
523 *et al.* Targeting colorectal cancer via its microenvironment by inhibiting IGF-1
524 receptor-insulin receptor substrate and STAT3 signaling. *Oncogene* 2016; **35**:
525 2634-44.

526 Secrier M, Li X, de Silva N, Eldridge MD, Contino G, Bornschein J, *et al.* Mutational
527 signatures in esophageal adenocarcinoma reveal etiologically distinct subgroups
528 with therapeutic relevance. *Nat Genet* 2016; **48**: 1131-41.
529 Smith TA. Mammalian hexokinases and their abnormal expression in cancer. Br J *Biomed*
530 *Sci* 2000; **57**: 170–8.
531 Straussman R, Morikawa T, Shee K, Barzily-Rokni M, Qian ZR, Du J, *et al.* Tumour micro-
532 environment elicits innate resistance to RAF inhibitors through HGF secretion.
533 *Nature* 2012; **487**: 500-4.
534 Tao L, Huang G, Song H, Chen Y, Chen L. Cancer associated fibroblasts: An essential
535 role in the tumor microenvironment. *Oncol Lett* 2017; **14**: 2611-20.
536 Takahashi H, Sakakura K, Kudo T, Toyoda M, Kaira K, Oyama T, *et al.* Cancer-associated
537 fibroblasts promote an immunosuppressive microenvironment through the
538 induction and accumulation of protumoral macrophages. *Oncotarget 2017;* **8**: 8633-
539 47.
540 Torres S, Bartolomé RA, Mendes M, Barderas R, Fernandez-Aceñero MJ, Peláez-García
541 A, *et al.* Proteome profiling of cancer-associated fibroblasts identifies novel
542 proinflammatory signatures and prognostic markers for colorectal cancer. *Clin*
543 *Cancer Res 2013;* **19**: 6006-19.
544 Trinchieri G. Cancer and inflammation: an old intuition with rapidly evolving new concepts.
545 *Annu Rev Immunol* 2012; **30**: 677-706.
546 Underwood TJ, Hayden AL, Derouet M, Garcia E, Noble F, White MJ, *et al.* Cancer-
547 associated fibroblasts predict poor outcome and promote periostin-dependent
548 invasion in oesophageal adenocarcinoma. *J Pathol* 2015; **235**: 466-77.
549 Van Berlo JH, Voncken JW, Kubben N, Broers JL, Duisters R, van Leeuwen RE, *et al.* A-
550 type lamins are essential for TGF-beta1 induced PP2A to dephosphorylate
551 transcription factors. *Hum Mol Genet* 2005; **14**: 2839-49.

552 Wang C, Xi W, Jiang J, Ji J, Yu Y, Zhu Z, *et al.* Metronomic chemotherapy remodel
553 cancer-associated fibroblasts to decrease chemoresistance of gastric cancer in
554 nude mice. *Oncol Lett 2017;* **14**: 7903-9.
555 Weaver JMJ, Ross-Innes CS, Shannon N, Lynch AG, Forshew T, Barbera M, *et al.*
556 Ordering of mutations in preinvasive disease stages of esophageal carcinogenesis.
557 *Nat Genet* 2014; **46**: 837-43.
558 Wen X, He X, Jiao F, Wang C, Sun Y, Ren X, *et al.* Fibroblast Activation Protein-α-Positive
559 Fibroblasts Promote Gastric Cancer Progression and Resistance to Immune
560 Checkpoint Blockade. *Oncol Res* 2017; **25**: 629-40.
561 Woodson K, Flood A, Green L, Tangrea JA, Hanson J, Cash B, *et al.* Loss of insulin-like
562 growth factor-II imprinting and the presence of screen-detected colorectal
563 adenomas in women. *J Natl Cancer Inst* 2004; **96**: 407-10.
564 Yeh CR, Slavin S, Da J, Hsu I, Luo J, Xiao GQ, *et al.* Estrogen receptor α in cancer
565 associated fibroblasts suppresses prostate cancerinvasion via reducing CCL5, IL6
566 and macrophage infiltration in the tumor microenvironment. *Mol Cancer* 2016; **15**:
567 7.
568 Zeidan B, Jackson TR, Larkin SE, Cutress RI, Coulton GR, Ashton-Key M, *et al.* Annexin
569 A3 is a mammary marker and a potential neoplastic breast cell therapeutic target.
570 *Oncotarget* 2015; **6**: 21421-7.

**Declaration:** The authors have no conflict of interest to declare

**Funding**: Wessex Cancer Trust, CRUK – Southampton Internal Pilot Grant, EU-FP7 Marie Curie (CANOMICS), Annual Adventures in Research – University of Southampton, EU-Excellence II – Systems Biology Framework FRA-SYS (Grant 4072).

**Authors' contributions**: A.M. and A.H. designed study, performed experiments, interpreted results and wrote manuscript; M.M. interpreted results and edited manuscript; D.J.G.B., provided analytic tools; C.H.W. performed biostatistical analysis; F.N. and M.L. sample procurement; G.J.T. interpreted results and edited manuscript, T.J.U. and S.D.G. raised funding, designed study, interpreted results and wrote manuscript.

**Acknowledgements:** We are indebted to Mr. Roger Allsopp, Mr. Derek Coates and Hope for Guernsey for establishing the clinical mass spectrometry infrastructure at the University of Southampton. The authors are grateful to the support of King Saud University, Deanship of Scientific Research Chair, Prince Mutaib Bin Abdullah Chair for Biomarkers of Osteoporosis, College of Science, as well as the Visiting Professor Program of King Saud University, Riyadh, Saudi Arabia.

599 **Figure Legends**

600

601 **Figure 1.** Study workflow

602

603 **Figure 2.** (A) Principal component analysis using the reporter ion log2ratios of all analysed
604 proteins showed that CAF have a distinct proteomic profile and higher heterogeneity
605 compared to NOF. (B) Volcano plot highlighting the differentially expressed proteins in
606 CAF vs. NOF (red=up-regulated proteins; green=down-regulated proteins). (C) Alpha
607 smooth muscle actin (ACTA2) was found to be significantly up-regulated in CAF vs. NOF
608 (Mean log2ratio (SD) = 0.2 (0.9); p-value < 0.0001 at the peptide level) (D) In total, 136
609 DEPs were also analysed with the same trend of modulation in a previously published
610 proteomics dataset of primary CAF/NOF cells from patients with OAC. Of these five up-
611 and 11 down-regulated proteins were confirmed in the microarray dataset (highlighted in
612 grey).

613

614 **Figure 3.** (A) The diseases and functions module of IPA predicted the significant inhibition
615 of *Adhesion of Epithelial Cells* (z-score = - 2.4 | p=6.3E-06), *Adhesion of connective tissue*
616 *cells* (z-score = - 2.3 | p=1.8E-05) and *Cell death of Fibroblast Cell Lines* (z-score = - 2.2 |
617 p=1.7E-09) in CAFs vs. NOFs. (B) KEGG pathway analysis using DAVID showed a
618 significant enrichment of the insulin-signalling pathway (Fisher exact p-value= 0.03 for the
619 common proteins between the two proteomics experiments and 0.05 for the DEPs
620 analysed in the present study).

621

622 **Figure 4.** (A) DAVID gene ontology analysis showed that gene ontology terms related with
623 *Myofibroblast phenotype*, *Metabolism*, *Cell adhesion/migration*, *Hypoxia/oxidative stress*,
624 *Angiogenesis*, *Immune/inflammatory response* were significantly over-represented in the
625 DEP. (B) Heatmap of top 10 up- and top 10 down-regulated proteins mapping to each
626 gene ontology terms category. The subcellular location of each protein is also presented

627 and up-regulated proteins that are either secreted or membrane are highlighted as
628 potential therapeutic targets.
629
630 **Figure 5.** (A) Using the *in silico* PrognoScan meta-analysis microarray database, higher
631 expression levels of nestin was found to correlate with poor patient prognosis [COX p-
632 value=0.003; HR (95% CI) = 78.0 (4.3 to 1409.8)]. (B) Immunohistochemical staining of
633 nestin in OAC showed a conserved expression pattern in the tumour microenvironment,
634 with expression being confined to CAF, blood vessels and smooth muscle cells.
635

Figure 1

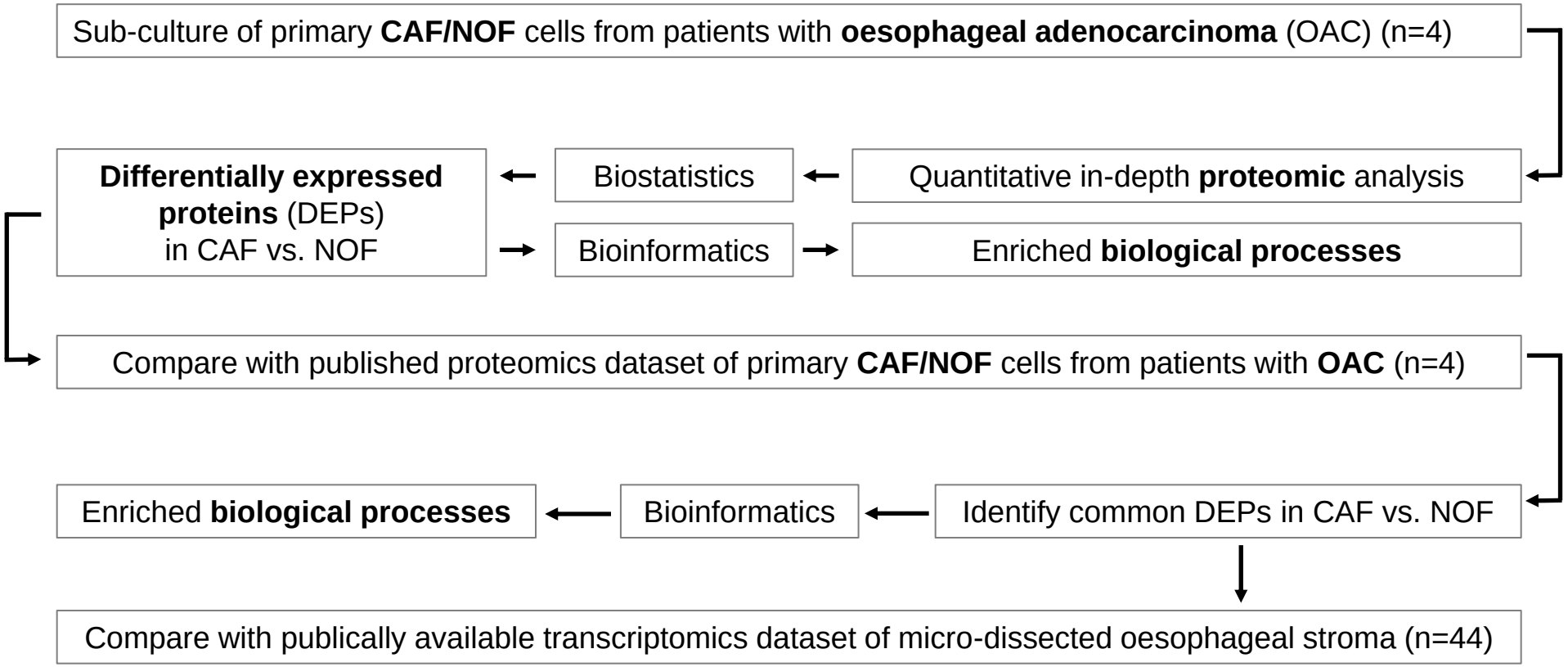
Sub-culture of primary **CAF/NOF** cells from patients with **oesophageal adenocarcinoma** (OAC) (n=4)
Quantitative in-depth **proteomic** analysis
Biostatistics
**Differentially expressed proteins** (DEPs) in CAF vs. NOF
Bioinformatics
Enriched **biological processes**
Compare with published proteomics dataset of primary **CAF/NOF** cells from patients with **OAC** (n=4)
Identify common DEPs in CAF vs. NOF
Bioinformatics
Enriched **biological processes**
Compare with publically available transcriptomics dataset of micro-dissected oesophageal stroma (n=44)

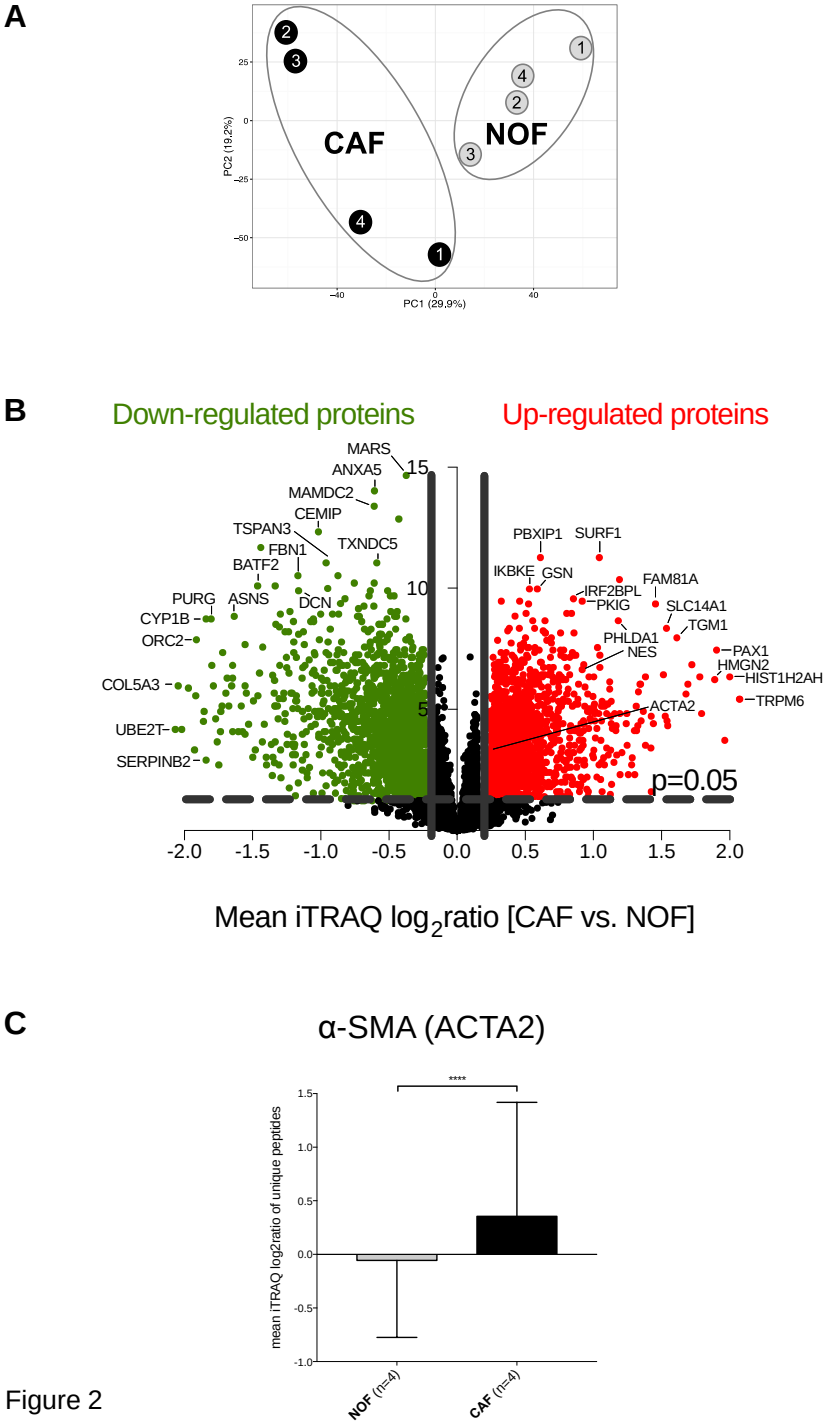


| Proteomics A | Proteomics B | Microarray GSE19632 | Gene name | Subcellular location |
|---|---|---|---|---|
| | | | SDPR | C |
| | | | NES | EC \| CS |
| | | | SVIL | M \| CS |
| | | | CSPG4 | M |
| | | | CTSZ | L |
| | | | LNP | ER |
| | | | S100A10 | EC |
| | | | ALB | EC |
| | | | PMVK | P |
| | | | EHD2 | E \| C \| M |
| | | | CAV1 | M \| G |
| | | | PALLD | CS |
| | | | LMNA | N |
| | | | ESYT1 | M \| ER |
| | | | LMNB2 | N |
| | | | SFPQ | N |
| | | | PTRF | M \| C \| N |
| | | | HK1 | Mit |
| | | | GSTK1 | P |
| | | | HNRNPL | N |
| | | | INF2 | C |
| | | | TPR | CS \| N |
| | | | PLEC | CS |
| | | | AARS2 | Mit |
| | | | GLUD1 | Mit |
| | | | TJP1 | M |
| | | | IVD | Mit |
| | | | ACADVL | Mit |
| | | | ACTA2 | CS |
| | | | DHX9 | CS \| N |
| | | | CD44 | M |
| | | | GALNS | L |
| | | | PDLIM5 | M |
| | | | ACTN4 | N |
| | | | ACTN1 | C \| CS |
| | | | FAM129B | C |

| Proteomics A | Proteomics B | Microarray GSE19632 | Gene name | Subcellular location |
|---|---|---|---|---|
| | | | RHEB | ER \| C \| G |
| | | | LONP1 | Mit |
| | | | MTPN | N |
| | | | HSPA5 | ER |
| | | | FASN | C |
| | | | RPL28 | EC \| C |
| | | | MAP2K2 | M \| C |
| | | | DNAJB11 | ER |
| | | | PNPO | EC \| C \| N |
| | | | M6PR | L |
| | | | OPTN | G \| E |
| | | | LMAN1 | ER \| G |
| | | | MAPK3 | N |
| | | | NAGK | EC \| C |
| | | | SSR1 | ER |
| | | | EEA1 | E |
| | | | VPS26A | E |
| | | | UQCRFS1 | Mit |
| | | | PRKG1 | C |
| | | | RPL18A | C |
| | | | APP | M |
| | | | UCHL3 | C |
| | | | EIF2S1 | N |
| | | | LDHB | C |
| | | | ARFGAP3 | G |
| | | | ATP6V1F | EC \| C |
| | | | ERP44 | ER |
| | | | ABHD14B | N |
| | | | RPS26 | EC \| C \| N |
| | | | RELA | N |
| | | | TXNRD1 | N |
| | | | TMX1 | ER |
| | | | PEPD | EC |
| | | | CLCN7 | L |
| | | | DARS | C |
| | | | EPS15 | M \| E |
| | | | EEF2 | N |
| | | | FSCN1 | C \| CS |
| | | | NUDCD1 | N |
| | | | VAT1 | Mit |
| | | | CKAP4 | M \| CS \| ER |
| | | | GBE1 | EC \| C |
| | | | ACSL3 | ER \| P \| Mit |
| | | | ATP2B1 | M |
| | | | ABCE1 | Mit |
| | | | IL6ST | EC \| M |
| | | | EIF5B | C |
| | | | FAM114A2 | N |
| | | | AGL | C |
| | | | DDR2 | M |

| Proteomics A | Proteomics B | Microarray GSE19632 | Gene name | Subcellular location |
|---|---|---|---|---|
| | | | MARS | C |
| | | | LTA4H | C |
| | | | ACOT1 | C |
| | | | NDUFV1 | Mit |
| | | | TARS | C |
| | | | EIF5A | ER \| N |
| | | | LAMP1 | M \| L \| E |
| | | | FAU | EC \| C \| N |
| | | | REXO2 | Mit \| N |
| | | | PPA1 | C |
| | | | LASP1 | CS |
| | | | NDUFA2 | Mit |
| | | | RCN1 | ER |
| | | | HS2ST1 | G |
| | | | ATP6V0D1 | M |
| | | | RNH1 | C |
| | | | PSMB7 | N |
| | | | XPNPEP1 | C |
| | | | CARS | C |
| | | | FKBP7 | ER |
| | | | UBE2K | C |
| | | | PDXDC1 | G |
| | | | IGF2R | L |
| | | | NARS | C |
| | | | MMP14 | M |
| | | | PEA15 | C |
| | | | MIEN1 | M \| C |
| | | | PGRMC2 | M |
| | | | TMX3 | ER |
| | | | SLC1A5 | M |
| | | | RPL35A | EC \| M \| C |
| | | | STX6 | G |
| | | | ANXA5 | EC \| C |
| | | | TM9SF2 | E |
| | | | TOM1 | M \| C |
| | | | YARS | C |
| | | | WARS | C |
| | | | UCHL1 | ER |
| | | | NPC1 | E \| L |
| | | | CCPG1 | M |
| | | | MMP2 | EC \| Mit \| N |
| | | | DAB2 | C |
| | | | MYH10 | C |
| | | | LAMP2 | M \| L \| E |
| | | | GARS | EC |
| | | | ALDH1L2 | Mit |
| | | | FTL | EC \| C \| L |
| | | | ADH1B | C |
| | | | PCK2 | Mit |
| | | | CYP1B1 | ER \| Mit |

Figure 2

**A**

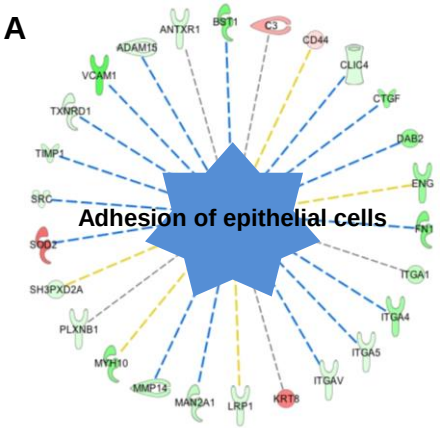


***z-score*** = - 2.4 | ***p-value*** =6.3E-06

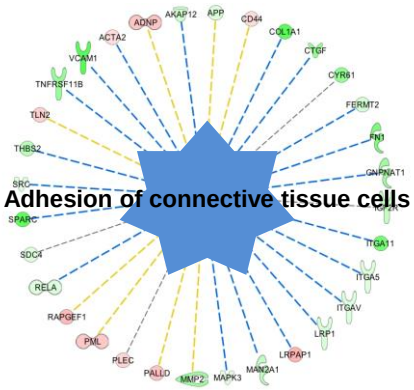


***z-score*** = - 2.3 | ***p-value***=1.8E-05

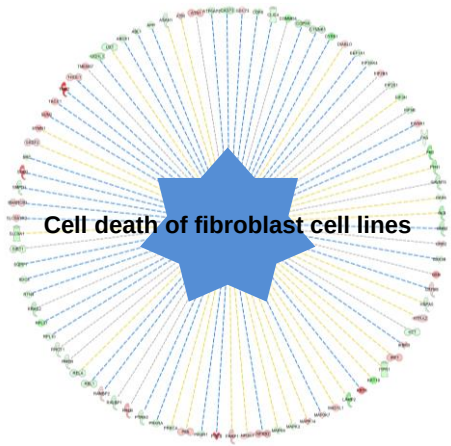


***z-score*** = - 2.2 | ***p-value***=1.7E-09

| Key | |
|---|---|
| up-regulated in CAF vs. NOF | Leads to inhibition |
| down-regulated in CAF vs. NOF | Finding inconsistent with effect |
| Predicted inhibition | Effect not predicted |

**B**

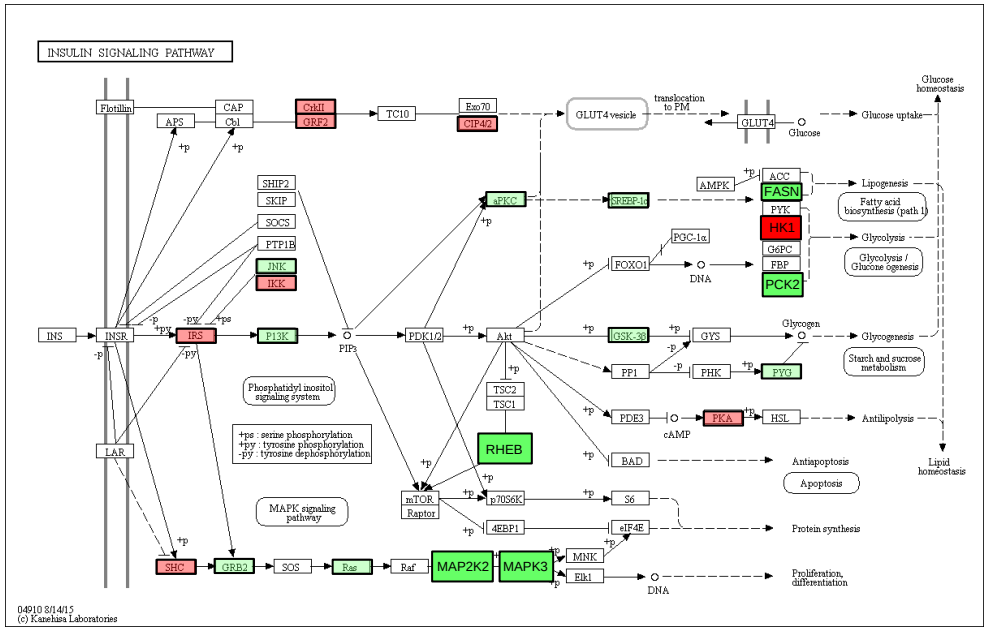


Fisher exact p-value= 0.05 in DEPs of present study and 0.03 in common DEPs with published proteomics dataset

| Key | |
|---|---|
| Proteins analyzed in present study | |
| up-regulated in CAF vs. NOF | up-regulated in CAF vs. NOF |
| down-regulated in CAF vs. NOF | down-regulated in CAF vs. NOF |

**A**

## Gene ontology enrichment analysis of DEPs in CAF vs. NOF

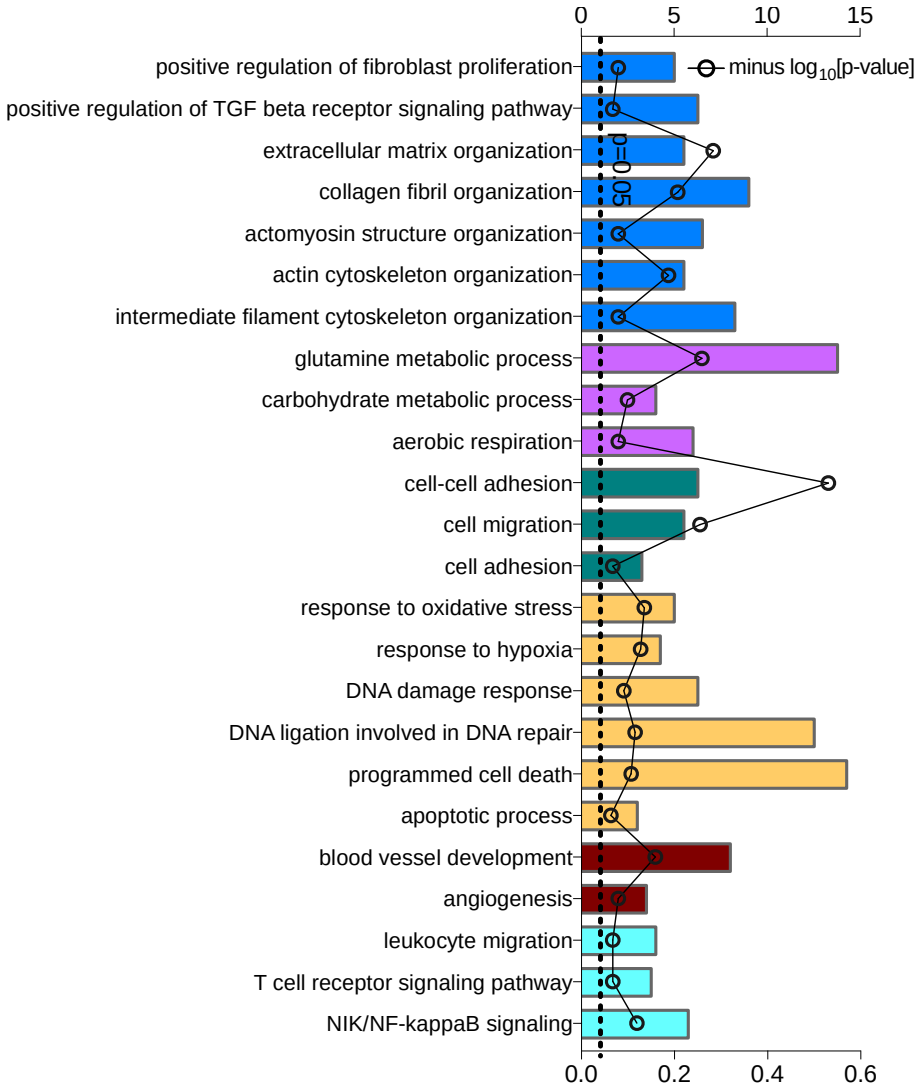


**GO term groups** (colour key)

- Myofibroblast phenotype
- Hypoxia/oxidative stress
- Metabolism
- Angiogenesis
- Cell adhesion/migration
- Immune/inflammatory response

**B**

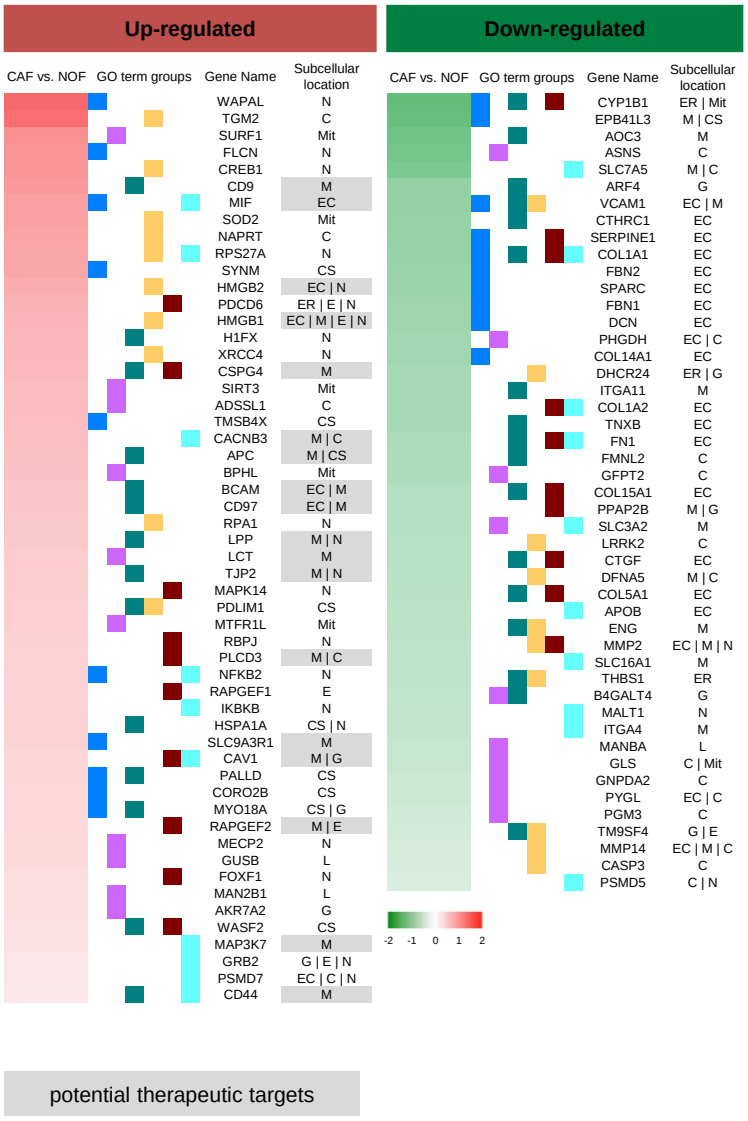


potential therapeutic targets

Abbreviations

**EC** = Extracellular region
**M** = Membrane
**C** = Cytosol
**CS** = Cytoskeleton
**ER** = Endoplasmic reticulum
**G** = Golgi apparatus
**L** = Lysosome
**E** = Endosome
**Mit** = Mitochondrion
**N** = Nucleus

Figure 4

**Nestin**

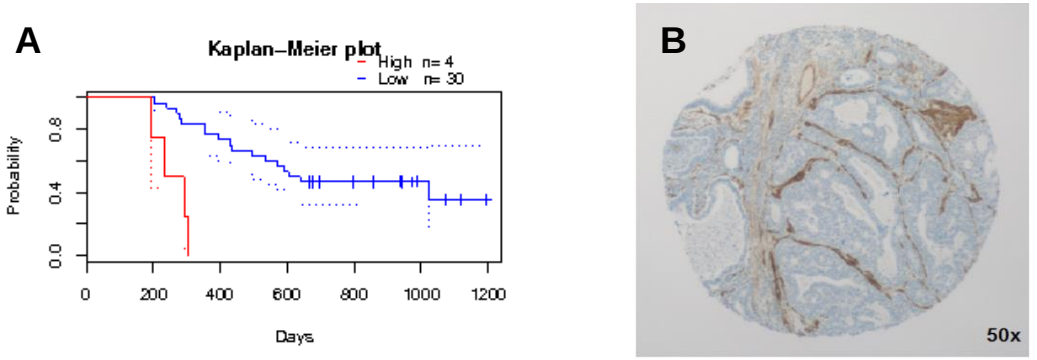


**Oesophageal adenocarcinoma**

Figure 5